

Transport of argon ions in an inductively coupled high-density plasma reactor

Citation for published version (APA):

Sadeghi, N., Griff, van de, M., Vender, D., Kroesen, G. M. W., & Hoog, de, F. J. (1997). Transport of argon ions in an inductively coupled high-density plasma reactor. *Applied Physics Letters*, 70(7), 835-837.
<https://doi.org/10.1063/1.118218>

DOI:

[10.1063/1.118218](https://doi.org/10.1063/1.118218)

Document status and date:

Published: 01/01/1997

Document Version:

Publisher's PDF, also known as Version of Record (includes final page, issue and volume numbers)

Please check the document version of this publication:

- A submitted manuscript is the version of the article upon submission and before peer-review. There can be important differences between the submitted version and the official published version of record. People interested in the research are advised to contact the author for the final version of the publication, or visit the DOI to the publisher's website.
- The final author version and the galley proof are versions of the publication after peer review.
- The final published version features the final layout of the paper including the volume, issue and page numbers.

[Link to publication](#)

General rights

Copyright and moral rights for the publications made accessible in the public portal are retained by the authors and/or other copyright owners and it is a condition of accessing publications that users recognise and abide by the legal requirements associated with these rights.

- Users may download and print one copy of any publication from the public portal for the purpose of private study or research.
- You may not further distribute the material or use it for any profit-making activity or commercial gain
- You may freely distribute the URL identifying the publication in the public portal.

If the publication is distributed under the terms of Article 25fa of the Dutch Copyright Act, indicated by the "Taverne" license above, please follow below link for the End User Agreement:

www.tue.nl/taverne

Take down policy

If you believe that this document breaches copyright please contact us at:

openaccess@tue.nl

providing details and we will investigate your claim.

Transport of argon ions in an inductively coupled high-density plasma reactor

N. Sadeghi^{a)}

Laboratoire de Spectrométrie Physique (UMR CNRS 5588), Université Joseph Fourier de Grenoble I, 38402 Saint Martin d'Hères Cedex, France

M. van de Grift,^{b)} D. Vender, G. M. W. Kroesen, and F. J. de Hoog

Department of Applied Physics, Eindhoven University of Technology, 5600 MB Eindhoven, the Netherlands

(Received 17 October 1996; accepted for publication 10 December 1996)

The first direct observation of the velocity distribution of the metastable $\text{Ar}^{+*}(^2G_{9/2})$ ions in the presheath of an inductively coupled plasma has been achieved by using the Doppler shifted laser induced fluorescence technique. Drift of the ions along the electric field in the presheath is observed and distribution functions of the velocity in both parallel and perpendicular directions, relative to the E field, are deduced at 5 and 40 mTorr. Present results show that in high density plasmas the velocity distribution of the metastable ions is directly related to that of the ground state argon ions. Neutral gas temperature of around 600 K is also measured from the absorption profile of a diode laser beam, set on one of the 772.4 nm argon lines. © 1997 American Institute of Physics. [S0003-6951(97)03707-8]

The need for rapid and large area wafer processing in the semiconductor industry has increased the interest in high density plasma sources and particularly in the inductively coupled plasma (ICP) reactors.¹ To fully exploit the possibilities in these reactors, of independent control of plasma generation and wafer biasing, we need to understand how ions are formed and how they gain energy before impinging on the wafer surface. Typically, the ICP is operated at pressure range 1–100 mTorr and powers of 200–2000 W, generating plasma with electron densities of 10^{11} – 10^{12} cm^{-3} and T_e 's of a few eV. Under these conditions, the sheath is collisionless and the dispersion of the velocity of ions when they hit the wafer surface is directly related to that present in the presheath–sheath boundary. Therefore, the knowledge of the ion velocity distribution function (ivdf) inside the presheath can give an insight into the transport of the ions from the plasma to the boundary surfaces. In general, the dimension of the presheath and the potential drop across it depend on the mean free path for ion-neutral collisions or electron-neutral ionization, and on the electron temperature. A review article by Riemann² provides a detailed kinetic treatment of the presheath. Recent simulations of ICP also give the evolution of the different plasma parameters inside the presheath.^{3,4} Experimentally, the parallel and transverse (to the B-field direction) ivdf have been measured downstream of an electron cyclotron resonance (ECR) argon plasma by using the Doppler-shifted laser induced fluorescence (DSLIF) technique.⁵ A Langmuir probe has also been used for the electrical diagnostics of the presheath in ECR⁶ and ICP.^{7–9} In this letter we report the direct measurement, by DSLIF, of the velocity distribution function of the argon ions in an ICP device. Both ivdf parallel and perpendicular to a glass plate limiting the plasma volume have been deter-

mined. We also measured the neutral gas temperature from the Doppler width of an absorption line of the argon metastable atoms.

Figure 1 shows a schematic diagram of the plasma reactor. The three turn, $\phi=10$ cm, inductive coil is located below a 12-mm-thick quartz window and is powered at 13.56 MHz with a 2 kW rf generator through an L-type capacitive matching network. The value of rf power quoted in this work is that applied to the matching network and includes both power dissipated in the plasma as well as the external components. We applied the same current through the inductive coil with and without plasma and measured the difference in applied power. In this way we can determine the losses in the matching network and other components and estimate the actual power dissipated in the plasma.⁷ At 400 W applied power, 40% (160 W) is absorbed in the plasma at 40 mTorr and 32% (128 W) at 5 mTorr. The $\phi=15$ cm Pyrex bucket which contains the plasma is located inside a $\phi=26.2$ cm,

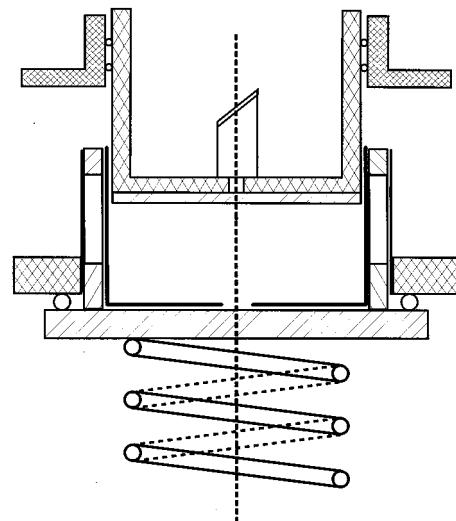


FIG. 1. Schematic of the ICP reactor.

^{a)}Electronic mail: nader.sadeghi@ujf-grenoble.fr

^{b)}Electronic mail: vdgrift@discharge.phys.tue.nl

$l=20.6$ cm high, vacuum vessel. A chromium coated copper cylinder, radially slatted in its base, is inserted into the bucket to insure Faraday shielding. A Pyrex plate is also inserted in the upper side of the bucket to limit the plasma volume to a $\phi=15$ cm, $l=3.8$ cm cylinder. To insure optical access and pressure equilibrium within the vessel, both bucket and metal cylinder have eight 6-mm-wide, 40-mm-high slits, located at 45° on their circumferences. For the DSLIF measurements we use a continuous wave single mode Ar^+ -pumped dye laser to excite the transition in $\text{Ar}^+(4p' \rightarrow 2F_{7/2}^0 \leftarrow 3d' \rightarrow 2G_{9/2})$ at 611.49 nm.⁵ Inside the reactor, the laser beam propagates along the reactor axis to observe $f(v_{\parallel})$, the ivdf parallel to the mean drift velocity of the ions toward the top glass plate, or along the diagonal to observe $f(v_{\perp})$, the ivdf parallel to the glass plate. The laser-induced fluorescence (LIF) signal, at 460.96 nm, is collected, at right angle to the laser directions, by a 10 cm focal length lens, located 20 cm from the reactor axis and is 1 to 1 imaged into a $\phi=1$ mm optical fiber bundle. Space resolution is therefore ± 0.5 mm in both axial and radial directions. The slit-shaped other end of the fiber is set in front of the entrance slit of a 60 cm Jobin Yvon HRS2 monochromator equipped with an R1617 Hamamatsu photomultiplier tube (PMT). To discriminate against the strong emission signal, the laser beam is modulated at 300 Hz, before entering the reactor, and the LIF signal is detected by using a lock-in amplifier. By tuning laser frequency and recording the LIF signal, we obtain the ivdf profile. For gas temperature measurements, we use a single mode diode laser, tuned on either 772.376 or 772.421 nm argon lines which can be absorbed by 3P_2 or 3P_0 metastable atoms, respectively.¹⁰ Before crossing the ICP reactor along a diagonal, the laser beam is attenuated to around $10 \mu\text{W}/\text{cm}^2$, to avoid saturation and optical pumping.¹¹ By tuning the diode laser frequency and recording the transmitted signal, we obtain the absorption profile of the line. The gas temperature is deduced from the Doppler width of the profile, which is a Gaussian for both lines. This supposes that due to the high efficiency of the elastic and metastability-exchange collisions, the metastable and ground state argon atoms have the same temperature.

The measured gas temperature, T_g , increases with the applied rf power. For our 400 W working power, we find that T_g increases slightly from 610 K, at 5 mTorr, to 650 K at 40 mTorr. The uncertainty of T_g is around 5%. T_g does not depend on the position of the laser beam relative to the top glass plate and is homogeneous within the plasma volume. Considering a pressure equilibrium between the vacuum vessel, where the capacitance manometer is located, and the ICP volume, T_g fixes the gas density inside the plasma.

Representative $f(v_{\parallel})$ distributions of argon metastable ions are shown in Fig. 2 for $p=5$ and 40 mTorr at different distances, d , from the top glass plate. Also shown is the $f(v_{\perp})$ at 5 mTorr and $d=12$ mm. Both velocity (bottom) and kinetic energy (top) scales are given. We observe that $f(v_{\perp})$ profile is symmetrical regarding the zero velocity and has almost a Gaussian shape. On the contrary, for both pressures $f(v_{\parallel})$ profiles cannot be fitted with a Gaussian. We also observe that $f(v_{\parallel})$ shifts to higher velocity when approaching the glass plate. Let us express, as usual,¹² the random

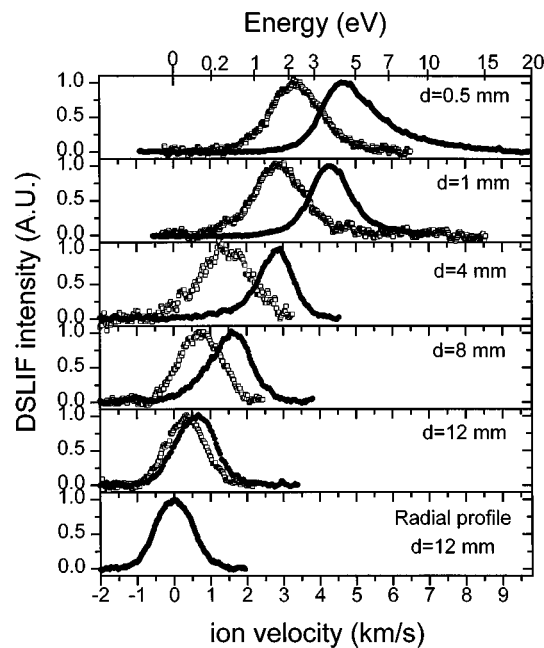


FIG. 2. Velocity distribution function of the $\text{Ar}^{+*}(^2G_{9/2})$ ions at different distances from the top glass plate at pressures 5 (solid circle) and 40 (hollow square) mTorr. All profiles are normalized to unity. The five upper pair of curves are relative to the velocity components along the reactor axis and the lowest curve corresponds to the velocity component parallel to the glass plate.

velocity partition in terms of temperatures and the mean drift energy

$$kT_{\perp} = M \langle (v_{\perp} - \langle v_{\perp} \rangle)^2 \rangle / e, \quad (1)$$

$$kT_{\parallel} = M \langle (v_{\parallel} - \langle v_{\parallel} \rangle)^2 \rangle / e, \quad (2)$$

$$E_{\parallel} = 1/2 M \langle v_{\parallel}^2 \rangle / e, \quad (3)$$

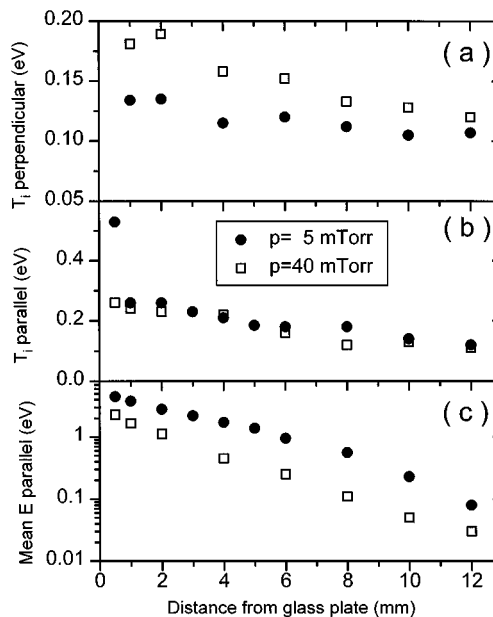


FIG. 3. Variation, vs the distance from glass plate, of the mean kinetic energy of the $\text{Ar}^{+*}(^2G_{9/2})$ ions along the reactor axis (c), of the parallel temperature T_{\parallel} (b), and perpendicular temperature T_{\perp} (a) at pressures 5 (solid circle) and 40 (hollow square) mTorr.

where M is the mass of the argon ion and $kT_{\perp}, kT_{\parallel}$, and E_{\parallel} are expressed in eV. Figure 3 summarizes the evolution of these quantities as a function of the distance from the glass plate. The almost exponential increase of E_{\parallel} when approaching the glass plate results from the acceleration of the ions by the electric field of the presheath. It is important to remember that E_{\parallel} corresponds to the mean drift energy of the ions in metastable state $\text{Ar}^{+*}(^2G_{9/2})$, which represents less than 1% of the total argon ion density.¹³ To see how these data are representative of the ground state ions, it is necessary to consider mechanisms by which $\text{Ar}^{+*}(^2G_{9/2})$ ions are produced and destroyed. Given the large cross-section, $\sigma=1.1 \cdot 10^{-16} \text{ cm}^2$, for quenching of the $\text{Ar}^{+*}(^2G_{9/2})$ metastable ions by argon atoms,^{14,15} the mean free path of these ions will be 12 and 1.5 mm at 5 and 40 mTorr, respectively. We therefore can conclude that, particularly at 40 mTorr, the $\text{Ar}^{+*}(^2G_{9/2})$ metastable ions we detect by DSLIF are not those formed outside the presheath and accelerated within it, but are produced by electron impact, a few mm before their respective observation points. If the main mechanism for population of the $\text{Ar}^{+*}(^2G_{9/2})$ metastable state was direct ionization of the neutral atoms, we should observe a large zero velocity component in all ivdfs and particularly those recorded close to the glass plate. All ivdfs shown in Fig. 2 are free from this component. It is obvious that in our high electron density conditions, the $\text{Ar}^{+*}(^2G_{9/2})$ level is mainly populated by electron impact excitation of ground state argon ions. In fact, these ions have already gained kinetic energy by being accelerated by the ambipolar E field of the presheath and their velocity is totally conserved during electron impact excitation of the ion. This is a very important conclusion. It points out that the velocity distribution of the $\text{Ar}^{+*}(^2G_{9/2})$ metastable ions, detected by DSLIF, is representative of the velocity distribution of the ground state argon ions. This conclusion is in fact only correct for the high density plasmas with ionization degrees of a few percent. In high pressure plasmas, where usually the Ar^+/Ar density ratio is smaller than 10^{-5} , excitation from the ground state atoms becomes dominant.

As shown in Fig. 3(b), T_{\parallel} increases when approaching the glass plate boundary. We think that this enhancement mainly results from a spatial distribution of the ionization within the presheath. In fact, given the cross section for inelastic collisions of electrons ($\sigma \cong 3 \times 10^{-16} \text{ cm}^2$) their mean free path is much larger than l . Therefore, T_e is almost constant inside the plasma volume but the electron density inside the presheath should decay according to $n=n_0 \exp(-\phi/kT_e)$. Argon ions are then produced all along the presheath with zero E_{\parallel} and have different energy gain at

observation points close to the plate. We should point out that for small d , as seen from Fig. 2, the observed kinetic energy dispersion in the lab frame is much larger than T_{\parallel} , which is representative of the energy dispersion in the ion frame. The very large value of T_{\parallel} for $d=0.5 \text{ mm}$, $p=5 \text{ mTorr}$, and the high energy tail observed in Fig. 2 in the ivdf for these conditions, is due to the fact that given the 0.5 mm space resolution in these experiments, some part of the LIF signal comes from $\text{Ar}^{+*}(^2G_{9/2})$ ions inside the sheath. These ions have been accelerated inside the sheath and have gained velocities larger than the Bohm velocity.

We also observe [Fig. 3(a)] that T_{\perp} increases with pressure and when approaching the glass boundary. Nevertheless, it is always smaller than T_{\parallel} . This behavior of T_{\perp} is a consequence of the elastic and charge exchange collisions of the Ar^+ ions with Ar neutrals. Even though these collisions are preferentially forward scattering,¹⁶ some part of the kinetic energy gained by the ions drifting along the E field in the presheath is transferred to their transverse motion. The amount of this transferred energy depends in fact on both E_{\parallel} and gas pressure.

In conclusion, we showed that in high density plasmas the velocity distribution function of the metastable argon ions $\text{Ar}^{+*}(^2G_{9/2})$ is representative of the velocity of the ground state ions. We also measured both parallel and perpendicular ivdfs of these ions.

¹M. A. Liebermann and R. A. Gottscho, *Physics of Thin Films*, edited by M. Francombe and J. Vossen (Academic, New York, 1994), Vol. 18, pp 1–119.

²K.-U. Riemann, *J. Phys. D* **24**, 493 (1991).

³R. A. Stewart, P. Vitello, D. B. Graves, E. F. Jaeger, and L. A. Berry, *Plasma Sources Sci. Technol.* **4**, 36 (1995).

⁴G. DiPeso, V. Vahedi, D. W. Hewett, and T. D. Rognlien, *J. Vac. Sci. Technol. A* **12**, 1387 (1994).

⁵N. Sadeghi, T. Nakano, D. J. Trevor, and R. A. Gottscho, *J. Appl. Phys.* **70**, 2552 (1991).

⁶J. A. Mayer, G.-H. Kim, M. J. Goekner, and N. Hershkowitz, *Plasma Sources Sci. Technol.* **1**, 147 (1992).

⁷P. N. Wainman, M. A. Lieberman, A. J. Lichtenberg, R. A. Stewart, and C. Lee, *J. Vac. Sci. Technol. A* **13**, 2464 (1995).

⁸V. A. Godyak, R. B. Piejak, and B. M. Alexandrovich, *Plasma Sources Sci. Technol.* **4**, 332 (1995).

⁹L. J. Mahoney, A. E. Wendt, E. Barrios, C. J. Richards, and J. L. Shohet, *J. Appl. Phys.* **76**, 2041 (1994).

¹⁰W. L. Wiese, M. W. Smith, and B. M. Moles, *Natl. Stand. Ref. Data Ser. (U.S., Natl. Bur. Stand.)* **2**, 22 (1969).

¹¹R. E. Drullinger and R. N. Zare, *J. Chem. Phys.* **51**, 5532 (1969).

¹²H. R. Skullerud, *J. Phys. B* **9**, 535 (1976).

¹³K. P. Giapis, N. Sadeghi, J. Margot, R. A. Gottscho, and T. C. J. Lee, *J. Appl. Phys.* **73**, 7188 (1993).

¹⁴B. Pellissier and N. Sadeghi, *Rev. Sci. Instrum.* **67**, 3405 (1996).

¹⁵N. Sadeghi, F. Chatain, and J. Derouard (unpublished).

¹⁶R. N. Varney, H. Helm, E. Alge, H. Störis, and W. Lindinger, *J. Phys. B* **14**, 1695 (1981).